Published in final edited form as:
J Biol Chem. 2008 January 4; 283(1): 301–310. doi:10.1074/jbc.M705580200.

Mind Bomb-2 Is an E3 Ligase That Ubiquitinates the *N*-Methyl-D-aspartate Receptor NR2B Subunit in a Phosphorylation-dependent Manner[*,s]

Rachel Jurd[1], **Claire Thornton**[2], **Jun Wang**, **Ken Luong**, **Khanhky Phamluong**, **Viktor Kharazia**, **Stuart L. Gibb**, and **Dorit Ron**[3]
Gallo Research Center, Department of Neurology, University of California, San Francisco, Emeryville, California 94608

Abstract

The *N*-methyl-D-aspartate receptor (NMDAR) plays a critical role in synaptic plasticity. Post-translational modifications of NMDARs, such as phosphorylation, alter both the activity and trafficking properties of NMDARs. Ubiquitination is increasingly being recognized as another post-translational modification that can alter synaptic protein composition and function. We identified Mind bomb-2 as an E3 ubiquitin ligase that interacts with and ubiquitinates the NR2B subunit of the NMDAR in mammalian cells. The protein-protein interaction and the ubiquitination of the NR2B subunit were found to be enhanced in a Fyn phosphorylation-dependent manner. Immunocytochemical studies reveal that Mind bomb-2 is localized to postsynaptic sites and colocalizes with the NMDAR in apical dendrites of hippocampal neurons. Furthermore, we show that NMDAR activity is down-regulated by Mind bomb-2. These results identify a specific E3 ubiquitin ligase as a novel interactant with the NR2B subunit and suggest a possible mechanism for the regulation of NMDAR function involving both phosphorylation and ubiquitination.

The *N*-methyl-D-aspartate receptors (NMDARs)4 are glutamate-gated ion channels that are important in synaptic plasticity events in the mammalian brain, and are comprised of an obligatory NR1 subunit and modulatory NR2 (A–D) or NR3 subunits (1). While the NR1 subunit has a short intracellular tail, the NR2 subunits have large intracellular C-terminal tails that directly interact with proteins that play essential roles in the regulation of NMDAR function (2, 3).

The intracellular domains of NMDAR subunits are phosphorylated by a number of protein kinases. For example, Src-family protein-tyrosine kinases (PTKs), such as Src and Fyn, phosphorylate specific tyrosine sites within the NR2A and NR2B intra-cellular tails (4–7),

[*]This work was supported in part by the NIAAA, National Institutes of Health Grant R01AA013438-01A1 (to D. R.), the Alcoholic Beverage Medical Research Foundation (to D. R.), Swiss National Science Foundation (to R. J.), and the State of California for Medical Research on Alcohol and Substance Abuse through the University of California, San Francisco (to D. R.).

[s]The on-line version of this article (available at http://www.jbc.org) contains supplemental Fig. S1.

[3]To whom correspondence should be addressed: Gallo Research Center, 5858 Horton St., Suite 200, Emeryville, CA 94608. Tel.: 510-985-3150; Fax: 510-985-3101; dorit.ron@ucsf.edu.
[1]Present address: Dept. of Neuroscience, University of Pennsylvania, Philadelphia, PA.
[2]Present address: MRC Clinical Sciences Centre, Imperial College of Science Technology and Medicine, London, UK.

Supplemental Material can be found at: http://www.jbc.org/content/suppl/2007/10/26/M705580200.DC1.html

[4]The abbreviations used are: NMDAR, *N*-methyl-D-aspartate receptor; FynCA, constitutively active Fyn kinase; HEK, human embryonic kidney; LTP, long-term potentiation; Mib2, Mind bomb-2; PSD, postsynaptic density; UPS, ubiquitin-proteasome system; HA, hemagglutinin; GFP, green fluorescent protein; PI, phosphatidylinositol; aa, amino acids; MBP, maltose-binding protein.

and this positively modulates channel function (5, 7–12). Tyrosine phosphorylation of the NR2 subunits of the NMDAR is enhanced under a number of synaptic plasticity-related events, including long-term potentiation (LTP) (13–15), fear-related learning (16), exposure to alcohol (17–19), and ischemia (20).

Tyrosine phosphorylation also positively regulates the trafficking of NMDARs from intracellular compartments to the postsynaptic density (PSD) (10, 12), the stability of NMDARs at the synaptic membrane (21, 22) and controls the association of the NMDAR with spectrin (23). Tyrosine phosphorylation can also influence which proteins bind to the receptor. For example, phosphatidylinositol 3-kinase (PI 3-kinase), and phospholipase C-γ (PLC-γ) bind to NR2 subunits in a tyrosine phosphorylation-dependent manner (24, 25), and the increased association of PI 3-kinase with phosphorylated NMDARs has been suggested to contribute to altered signaling in the hippocampus after ischemia (20). Thus, tyrosine phosphorylation plays an essential role in both the regulation of NMDAR channel activity and NMDAR-mediated downstream signaling cascades.

In addition to phosphorylation, ubiquitination is another post-translational modification that plays an important role in regulating neuronal function. Ubiquitin is a 76-amino acid protein that covalently attaches to substrates in an ATP-dependent enzymatic reaction that requires the concerted efforts of E1, E2, and E3 ubiquitin ligases (26). E3 ubiquitin ligases are the critical components that generate specificity in the reaction via substrate recognition. While many cellular processes are known to involve ubiquitination, its involvement in neuronal synaptic plasticity has only recently been investigated. Hippocampal LTP requires a balance of both protein synthesis and ubiquitin-dependent degradation (27), and the stability of multiple proteins at the PSD is regulated by the ubiquitin-proteasome system (UPS) (28 – 30). Thus, both phosphorylation and ubiquitination are likely to be important regulators of NMDAR function.

Here we report the identification of the E3 ubiquitin ligase Mind bomb-2 (Mib2) as a novel NR2B subunit-interacting protein whose interaction with and ubiquitination of the NR2B subunit is enhanced in a Fyn phosphorylation-dependent manner. This leads to the down-regulation of NMDAR activity, suggesting a role for both phosphorylation and ubiquitination in NMDAR modulation.

EXPERIMENTAL PROCEDURES

Antibodies and Reagents

Affinity-purified rabbit polyclonal sera directed against a peptide sequence of mouse Mib2 (amino acids (aa) 429 – 443) was generated by New England Peptide (Gardner, MA) (Supplemental Fig. S1). Anti-Mib2 (mouse) antibodies were from Abnova (Taipei, Taiwan). Anti-NR2B (rabbit) antibodies were from Covance (Berkeley, CA). Anti-NR1 (mouse) and MAP2(a,b) and MAP2(a– c) (mouse) antibodies were from Chemicon (Temecula, CA). Anti-hemagglutinin (HA, rat) and alkaline phosphatase-conjugated digoxigenin antibodies were from Roche Applied Science (Indianapolis, IN), and anti-α-actinin (mouse) antibodies from Sigma. Anti-phosphotyrosine (mouse) and anti-Myc (mouse) antibodies were from Upstate (Lake Placid, NY) and anti-PSD-95 (mouse) antibodies were from Affinity Bioreagents (Golden, CO). Anti-NR2B (goat), NR1 (goat), actin (goat), HA (mouse), Fyn (rabbit and mouse), normal IgG and all horseradish peroxidase-labeled secondary antibodies were from Santa Cruz Biotechnologies (Santa Cruz, CA). Forskolin and MG-132 were purchased from Calbiochem, APV (2-amino-5-phosphonovaleric acid) was from Tocris (St. Louis, MO), and ketamine HCl was purchased from Henry Schein Inc (Palatine, IL).

Construction of Yeast Plasmids

The sequence encoding the cytoplasmic tail of human NR2B (ctNR2B; aa 839–1482) was amplified from cDNA derived from L(-tk) cells expressing human NR1 and NR2B (Merck, Sharp and Dohme, Harlow, UK), and subcloned into the multiple cloning site I (MCS-I) of the pBridge yeast expression plasmid (Clontech, Mountain View). Full-length human Fyn cDNA was amplified from Marathon Race-Ready human brain cDNA (Clontech) and sub-cloned into pGEM-T (Promega, Madison, WI). This construct (Fyn WT) was used as a template for site-directed mutagenesis of the tyrosine residue 531 to phenylalanine (Y531F), generating a constitutively active form of Fyn (FynCA). After verifying the point mutation by sequencing, FynCA was subcloned into the MCS-II of pBridge-ctNR2B. MCS-I of pBridge is under the control of a CMV promoter, whereas MCS-II is under the control of a conditional methionine promoter. Thus, ctNR2B is constitutively expressed from the pBridge-ctNR2B-FynCA construct, whereas FynCA expression is repressed in the presence of methionine in the growth media.

Yeast Three-hybrid Screening

An adult rat brain cDNA library in pACT2 (Clontech; “prey”) was screened using the pBridge-ctNR2B-FynCA plasmid for constitutive expression of the cytoplasmic tail of NR2B as “bait” and inducible expression of FynCA as the third component in the screen. The pBridge-ctNR2B-FynCA construct and cDNA library were sequentially co-transformed into AH109 yeast (Clontech) using standard techniques (31). Selection was performed using minimal media plus/minus methionine and colonies that were β-galactosidase positive in the absence of methionine (FynCA expressed) but β-galactosidase negative in the presence of methionine (FynCA repressed) were identified. The β-galactosidase assay was repeated on restreaked positive clones to confirm the initial result. Plasmid DNA from positive yeast colonies was isolated and sequenced.

Expression Constructs

Full-length human Mib2 cDNA (IMAGE clone 4341220) was purchased from ATCC (Manassas, VA) and subcloned into phCMV2 vector (Gene Therapy Systems; San Diego, CA) such that the 110-kDa Mib2 protein was fused in-frame with the N-terminal HA epitope. Similar constructs were made to express regions containing the zinc finger domain (aa 1–180), the ankyrin repeats (aa 504–855), and the RING finger domains (aa 857–1000) of Mib2. Each construct was verified by Western blot analysis using HA antibodies to detect the fusion protein after transient transfection of the cDNAs into HEK293 cells. The following cDNAs were kind gifts: GFP-NR2B, Robert Wenthold (National Institutes of Health, Bethesda, MD); NR2B and enhanced-GFP (eGFP), David Lovinger (National Institutes of Health, Bethesda, MD); NR1-1a, Michael Hollman (Ruhr University, Bochum, Germany); Myc-ubiquitin, Jennifer Johnston (Elan, South San Francisco, CA); maltose-binding protein (MBP), MBP-NR1 and MBP-NR2B constructs, Vivian Teichberg (Weizman Institute, Rehovot, Israel). MBP-NR2B was used as a template for site-directed mutagenesis of tyrosine residues 1252, 1336, and 1472 to aspartic acids (Y1252D, Y1336D, Y1472D), generating a phosphomimic mutant of NR2B that was verified by sequencing.

Recombinant Proteins

MBP-tagged proteins were expressed in *Escherichia coli*, affinity-purified, and immobilized on amylose resin according to the manufacturer’s protocol (New England Biolabs, Ipswich, MA).

In Vitro Translation

[^{35}S]methionine-labeled Mib2 was generated in rabbit reticulocyte lysates (TNT *in vitro* translation kit; Promega) using full-length Mib2 cDNA. *In vitro* translated products were analyzed by SDS-PAGE and fluorography.

In Vitro Binding Assays

The assay was performed as previously described (32). Results were visualized by autoradiography using the Typhoon PhosphorImager (Amersham Biosciences) and quantified by NIH Image 1.61. Purity of the recombinant proteins was verified by Coomassie staining.

Cell Culture

Human embryonic kidney (HEK293) cells were cultured on 10-cm plates in Dulbecco's modified Eagle's medium (Invitrogen, Carlsbad, CA) supplemented with 10% fetal bovine serum (HyClone, Logan, UT) and GIBCO™ MEM Non-Essential Amino Acids (Invitrogen). When cells reached 70% confluency, they were transiently transfected with cDNA constructs (up to 6 μg total) using Lipofectamine Plus (Invitrogen), in accordance with the manufacturer's instructions. The media was changed 24 h after transfection, and cells harvested 48 h after transfection.

For the preparation of primary hippocampal neurons, newborn rats (P0) were decapitated, and hippocampi were dissected bilaterally. Cells were dissociated by enzyme digestion with papain (Worthington, Lakewood, NJ) followed by brief mechanical trituration and plated on 2-chamber CC2 glass chamber slides (Nalge Nunc, Naperville, IL). Cells were plated (~1 × 10^5 cells/chamber) and maintained in Neurobasal medium supplemented with B27, penicillin, streptomycin, and Glutamax-1 (all from Invitrogen), and maintained in culture for up to 21 days.

Preparation of Cell Homogenates

HEK293 cells were harvested in PBS (1.5 mM KH_2PO_4, 8 mM Na_2HPO_4, 2.7 mM KCl, 137 mM NaCl), spun at 2000 rpm for 2 min, washed twice with phosphate-buffered saline, and resuspended in lysis buffer (50 mM Tris-HCl, pH 7.4, 10 mM EGTA, 10 mM EDTA, 320 mM sucrose, 1% deoxycholate), 1% SDS, and protease (Roche Applied Science) and phosphatase inhibitors (Sigma) per the manufacturer's instructions. Samples were sonicated briefly, and lysis was allowed to proceed for 30 min on ice. Following protein concentration determination (using a BCA kit, per manufacturer's instructions; Pierce), samples were diluted to 2 mg/ml with lysis buffer before proceeding with immunoprecipitation assays. Rat hippocampal slices and homogenates were prepared as previously described (5).

Immunoprecipitation Assays

Immunoprecipitation was performed with 5 μg of the appropriate antibodies and 500 μg of cell homogenate as previously described (5). Samples were resolved by SDS-PAGE and transferred to nitrocellulose membrane. Membranes were blocked in milk solution (5% milk, PBS, 0.05% Tween-20) except for the detection of phosphorylated proteins when a bovine serum albumin (BSA) solution (5% BSA, 200 mM Tris-HCl, pH 7.4, 0.9% NaCl, 0.1% Tween-20) was used. Membranes were incubated with the specific primary antibody, followed by incubation with horseradish peroxidase-conjugated secondary antibodies. Immunoreactivity was detected by enhanced chemiluminescence ECL (GE Health-care, Buckinghamshire, UK) and processed using the Typhoon PhosphorImager (Amersham Biosciences). Results were quantified by NIH Image 1.61.

Ubiquitination Assays

Cells were transiently transfected with cDNA constructs and were treated with the proteasome inhibitor MG-132 (42 μM) 3 h prior to homogenization. Cell homogenates and immunoprecipitations were prepared as described above, except that 42 μM MG-132 and 5 mM *N*-ethylmaledimide (Sigma) were added to all buffers. In addition, samples were diluted in lysis buffer containing 2% SDS to dissociate protein-protein interactions.

In Situ Hybridization

A fragment of the mouse Mib2 gene (aa 263–428) was generated by PCR using adult mouse brain cDNA (Clontech) as a template. The PCR product was sub-cloned into pGEM-T (Promega) and used as a template to generate sense and antisense digoxygenin-labeled riboprobes using the Digoxygenin RNA labeling kit (Roche Applied Science), as per the manufacturer's instructions. This sequence contained no significant homology to other known cDNAs, as determined by BLAST analysis. Hybridization was performed on 16–20 μm-thick sagittal cryostat sections as previously described (33). Digoxigenin antibodies conjugated to alkaline phosphatase were used at a concentration of 1:2,000, and the detection of alkaline phosphatase was performed with NBT/BCIP substrate according to the manufacturer's instructions (Roche Applied Science).

Immunocytochemistry

Rats were deeply anesthetized with an overdose of Euthasol® (Virbac, Forth Worth, TX) and perfused with 0.9% NaCl for 2 min, followed by 4% paraformaldehyde (PFA) for 10 min. Brains were removed, post-fixed in 4% PFA for 2 h, and sectioned (40 μm) using a vibratome. Free-floating sagittal sections were immunostained as previously described (33), using primary antibodies at the following concentrations: anti-Mib2 (rabbit; 1:500), anti-MAP2(a,b) (mouse; 1:500) and anti-NR1 (mouse; 1:500). Secondary antibodies were Cy3-labeled donkey anti-rabbit and FITC-labeled anti-mouse (1:250; Jackson ImmunoResearch, WestGrove, PA).

Primary hippocampal neurons were fixed in 4% PFA, followed by incubation in 3% normal donkey serum (Jackson ImmunoResearch) in PBS containing 0.1% Triton X-100 for 2 h at room temperature. Fixed neurons were incubated (overnight, 4 °C) in primary antibodies against Mib2 (1:250), MAP(a–c) (1:250), PSD-95 (1:100), or α-actinin (1:500,000) diluted in PBS/0.1% Triton X-100. Alexa Fluor-594 labeled donkey anti-rabbit and Alexa Fluor-488 labeled donkey anti-mouse secondary antibodies (Molecular Probes, Eugene, OR) were incubated for 2 h at room temperature, followed by washing 3× in phosphate-buffered saline/0.1% Triton X-100 and coverslipped using Vectashield mounting medium (Vector laboratories, Burlingame, CA). Images were acquired using the LSM 510 confocal microscope (Zeiss, Thornwood, NY).

Electrophysiology

HEK293 cells were transfected with cDNA constructs as described above, except that APV (500 μM) and ketamine (0.7 mM) were added to the media to prevent glutamate-induced excitatoxicity. 24 h after transfection, cells were reseeded at a density of 1×10^5 cells in 35-mm plates coated with 1% gelatin. 24 – 48 h after replating, one dish was transferred to the chamber of an upright microscope (BX50WI, Olympus, Tokyo, Japan) equipped with epifluorescent optics. Cells were continuously perfused with external solution that contained (in mM): 145 NaCl, 5.4 KCl, 1.8 $BaCl_2$, 15 HEPES, 10 glucose, 0.05 glycine, and 0.2 sodium orthovanadate (pH 7.3). When testing the effect of MG-132 (10 μM), we added it to the culture media 2–3 h before transferring cells to the recording chamber, and MG-132 (1 μM) was also present in the recording solution. Transfected cells were identified by the

fluorescence of eGFP that was co-transfected with the cDNA constructs. NMDA was dissolved into external solution daily at a concentration of 1 mM. Fast switching to NMDA-containing external solution was achieved by piezoelectric control of the lateral movement of a three-barrel square glass application pipette (SF-77B, Warner Instrument, CT). NMDA-elicited currents were measured at −60 mV in the whole cell voltage-clamp mode using Multiclamp 700A (Molecular Device, Union City, CA), as described previously (34). Recording electrodes (2–3 MΩ) were filled with internal solution containing (in mM): 121 cesium methanesulfate, 10 CsCl, 15 HEPES, 0.6 EGTA, 4 MgATP, 0.3 NaGTP, and 7 Na_2CrPO_4 (pH 7.25) with an osmolarity of 275 mOsm. Whole cell currents were low-pass filtered at 1 kHz and digitized at 2 kHz by Multicamp 700A software and pClamp 9 (Molecular Device, Union City, CA). Cell membrane capacitance was measured and compensated automatically. Series resistance was 50% compensated.

Statistical Analysis

All data are expressed as mean ± S.E. Electrophysiological results were analyzed by Student's *t* test. Biochemical results were analyzed using the one-sample *t* test or one-way analysis of variance, followed by *post-hoc* tests using Newman-Keuls method. Significance for all tests was set at $p < 0.05$.

RESULTS

Mib2 Interacts with the NR2B Cytoplasmic Tail in a Fyn-dependent Manner in Yeast

Because tyrosine phosphorylation of the NMDAR is a critical mechanism regulating channel activity and signal transduction (7), we designed a screen to identify proteins that interact with the NMDAR in a tyrosine phosphorylation-dependent manner. This yeast three-hybrid screen (35) consisted of a bait plasmid containing the cytoplasmic tail of NR2B (ctNR2B), prey proteins expressed from a rat brain cDNA library, and a constitutively active form of Fyn (FynY531F; FynCA (36)) whose expression was under the control of a conditional methionine promoter. In the presence of methionine in the growth media, FynCA expression was repressed. In the absence of methionine, FynCA expression was induced, and tyrosine phosphorylation of ctNR2B was observed (data not shown).

Approximately 5×10^5 independent transformant clones were screened in the absence and presence of methionine in the growth media. This resulted in the isolation of 32 colonies that were true three-hybrid interactants (*i.e.* interacted with ctNR2B only when FynCA was expressed; Fig. 1). Three of these colonies contained plasmids encoding the RING finger domain of Mib2, a protein that has previously been reported to have E3 ubiquitin ligase activity (37). Because of the recently identified role of the UPS in activity-dependent regulation of excitatory synaptic proteins (28–30), we were interested in further characterizing whether Mib2 was a phosphorylation-dependent NR2B-interacting protein.

Mib2 Interacts with the NR2B Subunit in a Phosphorylation-dependent Manner

Having identified the RING finger domain of Mib2 as a phosphorylation-dependent interactant with the cytoplasmic tail of NR2B in a yeast system, we next set out to determine whether this interaction occurs in mammalian cells. The RING finger domain of Mib2 was expressed as a HA-tagged protein together with GFP-tagged NR2B subunit in HEK293 cells, and the interaction between NR2B and this Mib2 domain was determined by immunoprecipitation. As shown in Fig. 2*A* (*lane 1*), anti-NR2B antibodies co-immunoprecipitated the RING finger domain of Mib2, indicating that the two proteins exist as a complex. IgG antibodies did not immunoprecipitate either NR2B or the RING finger domain, demonstrating the specificity of the observed interaction (Fig. 2*A*, *lane 2*).

Next, we determined whether the interaction between Mib2 and the NR2B subunit is regulated by Fyn phosphorylation. To do so, FynCA was transfected into HEK293 cells in addition to Mib2 and NR2B. Expression of FynCA in HEK293 cells resulted in robust tyrosine phosphorylation of the NR2B subunit (Fig. 2*A*, *lane 4 versus lane 1*, *top panel*). The association of the RING finger domain of Mib2 with NR2B showed a small, but significant, enhancement in the presence of FynCA (Fig. 2*A*, *lane 4 versus lane 1*, *bottom panel*, and Fig. 2*B*). However, transfection of full-length Mib2 into the same mammalian system resulted in a marked 2-fold increase in association in the presence of Fyn kinase (Fig. 2, *C* and *D*), suggesting that additional domains contained in the full-length protein contribute to its binding and regulated interaction with the NR2B subunit. Taken together, we show that the interaction between Mib2 and NR2B is significantly enhanced in a Fyn phosphorylation-dependent manner in mammalian cells.

To assess whether the interaction between NR2B and Mib2 is specific, we determined if Mib2 interacts with the NR1 obligatory subunit of the NMDAR. To do so, we expressed Mib2 together with NR1 in HEK293 cells. Anti-NR1 antibodies immunoprecipitated NR1, but failed to co-immunoprecipitate Mib2 (Fig. 2*E*), suggesting that Mib2 interacts specifically with NR2B, but not the NR1 subunit of the NMDAR.

Mib2 Interacts Directly with the Cytoplasmic Tail of NR2B

We next set out to determine if the interaction that we observed in mammalian cells was occurring through a direct protein-protein interaction between Mib2 and NR2B. Proteins encoding the C-terminal regions of the NR1 and NR2B subunit tagged with MBP were expressed in *E. coli* and incubated with *in vitro* translated radiolabeled Mib2 (^{35}S-Mib2). As shown in Fig. 3*A*, ^{35}S-Mib2 binds to MBP-NR2B (*lane 3*) but not to MBP-NR1 (*lane 2*) or the MBP tag alone (*lane 1*). Furthermore, ^{35}S-Mib2 bound strongly to a phosphomimic mutant form of MBP-NR2B (MBP-NR2B-mut) in which the three main sites of tyrosine phosphorylation by Src family kinases (Tyr^{1252}, Tyr^{1336}, Tyr^{1472}) have been mutated to aspartic acids to mimic constitutive phosphorylation (Fig. 3*A*, *lanes 4 versus 3*). ^{35}S-Mib2 was also observed to bind significantly more strongly to the distal portion of the NR2B C-terminal tail (encoded by MBP-2BΔN) compared with the more proximal part (MBP-2BΔC) (Fig. 3*B*, *lanes 2 versus 3*, and *C*). Thus, we have demonstrated that the binding of Mib2 to NR2B is a direct interaction and that it involves domains contained within the distal portion (aa 1170–1482) of the NR2B subunit (Fig. 3*D*).

The RING Finger and Ankyrin Domains of Mib2 Bind NR2B

Mib2 is a modular protein composed of RING-finger domains (RING) at its C terminus, a ZZ zinc finger (ZnF) domain and multiple ankyrin repeat domains (ANK) (Fig. 4*A*). RING finger domains are protein-protein interaction domains that have intrinsic ubiquitin ligase activity. The ZZ zinc finger domain is a putative zinc-binding domain, and ankyrin repeats are common protein-protein interaction motifs (SMART, simple modular architecture research tool). Our initial experiments in mammalian cells suggested that domains in addition to the RING finger may be responsible for Mib2 associating with the NR2B subunits (Fig. 2). Thus, to test which domains of Mib2 bind to the NR2B subunit, we expressed each of these domains as HA-tagged proteins, and expressed them in HEK293 cells together with GFP-NR2B. Immunoprecipitation experiments using anti-NR2B antibodies revealed that both the RING and ANK domains co-immunoprecipitate with NR2B, whereas the ZnF domain does not (Fig. 4*B*, *lane 1*, *bottom panel*). Therefore, binding of NR2B to Mib2 occurs through protein-protein interactions with the ankyrin and RING finger motifs.

Mib2 Colocalizes with NMDARs in Hippocampal Neurons

We next tested the mRNA and protein expression of Mib2 in the adult brain. We found that Mib2 is expressed in all major brain regions of the rat (data not shown), including the hippocampus (Fig. 5, *A–D*). Mib2 immunostaining was observed in apical dendrites of hippocampal CA1 pyramidal neurons, as evidenced by colocalization with the dendritic marker, MAP2 (Fig. 5*E*), and co-labeling studies using anti-NR1 antibodies revealed that Mib2 colocalizes with NMDARs in hippocampal apical dendrites (Fig. 5*F*). Next, to determine the subcellular localization of Mib2, we performed immunocytochemical experiments in cultured rat hippocampal neurons. Mib2 is located at synaptic sites, as evidenced by its punctate staining and co-localization with the postsynaptic marker PSD-95 (Fig. 6, *A* and *B*) and in dendritic spines, as revealed by α-actinin (Fig. 6*C*) and MAP2 stainings (Fig. 6*D*). Thus, Mib2 is an E3 ubiquitin ligase that localizes with NMDARs at postsynaptic sites in hippocampal dendrites. Mib2 associates with the NR2B subunit in the hippocampus. Next, we assessed whether Mib2 and NR2B associate in the brain and whether the association is dependent on phosphorylation. We previously showed that in hippocampal neurons, activation of the cAMP/PKA pathway leads to the phosphorylation of the NR2B subunit by Fyn (5). We therefore tested the association of Mib2 with NR2B in the presence or absence of the adenylate cyclase activator forskolin. As shown in Fig. 7, forskolin treatment resulted in an increase in NR2B phosphorylation (*lanes 1 versus 2*, *top panel*), and a corresponding increase in Mib2 co-immunoprecipitation with the NR2B subunit (*lanes 1 versus 2*, *bottom panel*). Similar results were obtained when KCl was added at the last 5 min of forskolin treatment to mimic brief neuronal stimulation (Fig. 7, *lanes 3 versus 1* and *2*). Together these results suggest that in the hippocampus, Mib2 binds NR2B in an activity-dependent manner.

Mib2 Ubiquitinates NR2B in a Fyn Phosphorylation-dependent Manner

Mib2 is known to have intrinsic E3 ubiquitin ligase activity (37). To test whether the NR2B subunit is a substrate for Mib2, we performed ubiquitination assays. Constructs encoding GFP-tagged NR2B, HA-tagged Mib2, FynCA, and Myc-tagged ubiquitin were co-expressed in HEK293 cells and immunoprecipitated with anti-NR2B antibodies, followed by immunoblotting with anti-Myc antibodies to detect ubiquitinated species of NR2B. A robust ubiquitinated signal for NR2B was seen when all constructs were co-expressed (Fig. 8*A*, *lane 4*), and this signal was significantly greater than in the absence of either Mib2 and/or Fyn-CA (Fig. 8*A*, *lanes 1*, *2*, *6*, and *8*, *B*). Together, these results demonstrate that ubiquitination of NR2B by Mib2 occurs in a Fyn phosphorylation-dependent manner.

We also addressed the question of whether Mib2 was capable of ubiquitinating the NR1 subunit, even though it did not directly associate with it (Fig. 2*E*). To do this, HA-Mib2, NR1 and myc-ubiquitin were co-expressed in HEK293 cells, followed by immunoprecipitation with anti-NR1 antibodies and immunoblotting with anti-Myc antibodies. No evidence for any ubiquitinated species of NR1 was observed (Fig. 8*C*). Thus, Mib2 selectively interacts with and ubiquitinates the NR2B subunit, but not the NR1 subunit, of NMDARs.

Mib2 Negatively Regulates the Functional Activity of NR2B-containing NMDARs in a Ubiquitin-Proteasome-dependent Manner

Thus far, we have demonstrated that Mib2 associates with and ubiquitinates the NR2B subunit of the NMDAR in a Fyn phosphorylation-dependent manner. To assess whether Mib2-mediated ubiquitination of NR2B results in altered channel activity, we measured NMDAR-mediated currents in HEK293 cells expressing NR1, NR2B, Myc-ubiquitin, and FynCA, in the presence and absence of Mib2. We found that expression of Mib2 significantly decreased the density of peak NMDAR-mediated currents (430 ± 93 pA/pF, *n*

= 13 cells *versus* 183 ± 30 pA/pF, n = 12 for cells without and with Mib2, respectively, $p < 0.05$; Fig. 9*A*). Furthermore, expression of a deletion mutant of Mib2 that is not capable of binding to NR2B (aa 1–180; ZnF, Fig. 4) does not affect NMDAR function (136 ± 56 pA/pF, n = 11 cells *versus* 145 ± 52 pA/pF, n = 12 for cells without and with ZnF, respectively, $p > 0.05$; Fig. 9*B*). Taken together with our observation that Mib2 ubiquitinates the NR2B subunit in the presence of FynCA (Fig. 8, *A* and *B*), these results suggest that Mib2 down-regulates the activity of NR2B-containing NMDARs via the ubiquitination of the NR2B subunit.

Finally, to determine whether this down-regulation of NMDAR function in the presence of Mib2 was dependent on the ubiquitin-proteasome system, the above experiments were repeated in the presence of the proteasome inhibitor, MG-132. In contrast to the Mib2-dependent decrease in NMDAR currents that was observed (Fig. 9*A*), we found that the preincubation of cells with MG-132 failed to produce a significant decrease in NMDAR-mediated currents (346 ± 75 pA/pF, n = 13 cells *versus* 361 ± 107 pA/pF, n = 14 cells, for cells without and with Mib2, respectively, $p > 0.05$; Fig. 9*C*). Together, these results suggest that inhibition of proteasomal function prevents the Mib2-mediated depression of NR2B-containing NMDAR function. Thus, Mib2 negatively regulates NR2B-containing NMDAR function in a ubiquitin-proteasome-dependent fashion.

DISCUSSION

Ubiquitination is emerging as a key regulatory mechanism in controlling the fate and function of neuronal proteins (28). However, not much is known about the particular substrates or ubiquitin enzymes involved in this process. In this article, we present findings that Mib2 is an E3 ubiquitin ligase that associates with and ubiquitinates the NR2B subunit of the NMDAR. We found that the interaction between Mib2 and the NR2B subunit is facilitated by Fyn kinase, suggesting that the association occurs in a phosphorylation-dependent manner. Furthermore, we demonstrate that the ubiquitination of the NR2B subunit by Mib2 is also Fyn kinase-dependent. Importantly, we show that Mib2 colocalizes with the NMDAR at postsynaptic sites and interacts with the NR2B subunit within hippocampal neurons. Finally we present data to suggest that the activity of the NMDAR is negatively regulated by Mib2 in a ubiquitin-proteasome-dependent manner.

In this study, we identify Mib2 as a protein whose association with the NR2B subunit is increased by Fyn phosphorylation. Relatively few studies have studied how NMDAR-protein interactions are dynamically regulated, such as by phosphorylation. PI 3-kinase and PLC-γ are two proteins that have been identified as interacting with NR2B subunits in a tyrosine phosphorylation-dependent manner (24, 25), while serine phosphorylation of NR2B has been demonstrated to regulate the interaction of PSD-95 with the NMDAR (38). These phosphorylation-dependent interactions are likely to play important roles in altering signaling via the NMDAR during processes such as synaptic plasticity (38) or during pathophysiological events (20). One plausible explanation for our current findings is that tyrosine phosphorylation of the NR2B subunit by Fyn leads to increased binding of Mib2 binding. The NR2B subunit is a known substrate for Fyn, and overexpression of FynCA was observed to lead to a significant increase in the level of tyrosine phosphorylation on the NR2B subunit. Furthermore, we observed association of Mib2 with NR2B in hippocampal slices after forskolin treatment, which induced the tyrosine phosphorylation of the NR2B subunit. Thus, Mib2 may serve a novel role in down-regulating the function of phosphorylated NR2B-containing NMDARs.

Tyrosine phosphorylation has generally been thought of as positively modulating NMDAR function (7), however the ubiquitination and down-regulation of NMDAR function that we

observed by Mib2 occurred in a Fyn kinase-dependent manner. We hypothesize that this negative regulation may be one mechanism that neurons use to avert the pathophysiological consequences of overactivation of the NMDAR, under circumstances in which Fyn activation and subsequent phosphorylation and positive modulation of the NMDAR would be detrimental if allowed to continue chronically. For example, to counterbalance excessive amounts of calcium entry through the channel that occurs during ischemia, due to up-regulation of tyrosine phosphorylation of NMDARs (20, 39). Interestingly, recently Wu *et al.* (40) reported that Fyn phosphorylation of the tyrosine 1336 residue on NR2B leads to calpain-mediated degradation of the subunit. Another possibility is that Mib2 may also be regulated by Fyn phosphorylation. The tyrosine phosphorylation of other E3 ligases, such as Cbl, has been shown to lead to enhanced binding and ubiquitination of the epidermal growth factor receptor (41). Furthermore, kinases such as cAMP-dependent protein kinase (PKA) and Src family PTKs are also regulated by the UPS (42). Hence, multiple levels of complexity in this system are possible, with our current findings not excluding the possibility that Mib2 is a target for regulation via Fyn phosphorylation, in addition to the NR2B subunit. Furthermore, Fyn may also potentially be modulated by ubiquitination. Dynamic regulation of the function of Mib2 or Fyn could affect the degree to which NR2B and Mib2 associate, and hence could be additional mechanisms that allow the level of NMDAR ubiquitination to be regulated in a temporally and spatially restricted manner.

Our finding that the NR2B subunit of the NMDAR is a substrate for Mib2 is interesting in light of other substrates that have previously been identified as associating with Mib2. The Notch ligand, Delta, is an integral membrane protein that associates with Mib2, resulting in its ubiquitination and down-regulation (37). Mib1, an E3 ligase that shares significant similarity to Mib2, has also been shown to ubiquitinate Delta (43, 44). Furthermore, a recent article has reported that Mib1 is localized to the PSD in hippocampal neurons (45). Here, we show that Mib2 is also localized to the PSD of hippocampal neurons. Thus both proteins are likely to play important roles in the ubiquitination of several neuronal proteins. Our identification of Mib2 as an E3 ligase that ubiquitinates the NR2B subunit does not rule out the possibility that other E3 ligases, in addition to Mib2, also function in this capacity, as five other E3 ligases are known to act in coordination with Mib2 to regulate the Notch-Delta signaling pathway (43, 46). Other E3 ligases, including Mdm2 and Parkin, have been demonstrated to reside at the PSD (30, 47). Furthermore, the ubiquitin-proteasome machinery is present in the dendrites of hippocampal neurons, with activity-dependent regulated movement of the proteasome from dendritic shafts to synaptic spines being observed (48). In addition, several ligand-gated ion channels, including mammalian glycine, $GABA_A$, and glutamate receptors, are known to be regulated by ubiquitination or sumoylation, a ubiquitin-like modification (49–52). However, phosphorylation-dependent ubiquitination of these receptors has not previously been reported and the exact nature of the ubiquitin machinery involved, especially the substrate specificity of synaptic E3 ligases, are questions that are only now starting to be addressed, and hence, will continue to be important issues for future research.

Abnormalities in the UPS pathway have been demonstrated in numerous neurological and neurodegenerative disorders (53), and large-scale changes in the expression of multiple genes involved in ubiquitination have been found in studies of alcoholics (54). Furthermore, mutations in the synaptically located E3 ligase Parkin have been associated with Parkinson's disease (55). The predominant localization of Mib2 at postsynaptic sites suggests that dysregulation in its function may also have significant consequences for neurological function. Conversely, regulated manipulation of Mib2 function may have important therapeutic implications, especially if selective modulation of NMDARs could be achieved. This could be particularly relevant for a number of neurological disorders, such as

schizophrenia, alcoholism, neuropathic pain, or ischemia, in which dysregulation of NMDAR function occurs (56–60).

In summary, the identification of Mib2 as an E3 ubiquitin ligase that binds to and ubiquitinates the NR2B subunit in a Fyn phosphorylation-dependent manner has significant implications for the negative regulation of NR2B-containing NMDARs.

Supplementary Material

Refer to Web version on PubMed Central for supplementary material.

Acknowledgments

We thank the following people for constructs and cell lines: Drs. R. Wenthold (National Institutes of Health, Bethesda, MD), M. Hollman (Ruhr University, Bochum, Germany), D. Lovinger (National Institutes of Health, Bethesda, MD), V. Teichberg (Weizman Institute, Rehovot, Israel), J. Johnston (Elan, South San Francisco, CA), and Merck, Sharp and Dohme (Harlow, UK). We thank R. Van Bautista, J. Srikantharajah, C. Santos, E. Wong, A. Eisner and S. Dinh for technical assistance and Dr. S. Carnicelli for statistical advice. We also thank Drs. J. Whistler and R.O. Messing for critically reading the manuscript.

References

1. Cull-Candy S, Brickley S, Farrant M. Curr Opin Neurobiol. 2001; 11:327–335. [PubMed: 11399431]
2. Wenthold RJ, Prybylowski K, Standley S, Sans N, Petralia RS. Annu Rev Pharmacol Toxicol. 2003; 43:335–358. [PubMed: 12540744]
3. Sheng M, Kim MJ. Science. 2002; 298:776–780. [PubMed: 12399578]
4. Suzuki T, Okumura-Noji K. Biochem Biophys Res Commun. 1995; 216:582–588. [PubMed: 7488151]
5. Yaka R, He DY, Phamluong K, Ron D. J Biol Chem. 2003; 278:9630–9638. [PubMed: 12524444]
6. Nakazawa T, Komai S, Tezuka T, Hisatsune C, Umemori H, Semba K, Mishina M, Manabe T, Yamamoto T. J Biol Chem. 2001; 276:693–699. [PubMed: 11024032]
7. Salter MW, Kalia LV. Nat Rev Neurosci. 2004; 5:317–328. [PubMed: 15034556]
8. Wang YT, Salter MW. Nature. 1994; 369:233–235. [PubMed: 7514272]
9. Kohr G, Seeburg PH. J Physiol (Lond). 1996; 492:445–452. [PubMed: 9019541]
10. Dunah AW, Standaert DG. J Neurosci. 2001; 21:5546–5558. [PubMed: 11466426]
11. Yaka R, Thornton C, Vagts AJ, Phamluong K, Bonci A, Ron D. Proc Natl Acad Sci U S A. 2002; 99:5710–5715. [PubMed: 11943848]
12. Hallett PJ, Spoelgen R, Hyman BT, Standaert DG, Dunah AW. J Neurosci. 2006; 26:4690–4700. [PubMed: 16641250]
13. Rosenblum K, Dudai Y, Richter-Levin G. Proc Natl Acad Sci U S A. 1996; 93:10457–10460. [PubMed: 8816822]
14. Lu YM, Roder JC, Davidow J, Salter MW. Science. 1998; 279:1363–1367. [PubMed: 9478899]
15. Rostas JA, Brent VA, Voss K, Errington ML, Bliss TV, Gurd JW. Proc Natl Acad Sci U S A. 1996; 93:10452–10456. [PubMed: 8816821]
16. Nakazawa T, Komai S, Watabe AM, Kiyama Y, Fukaya M, Arima-Yoshida F, Horai R, Sudo K, Ebine K, Delawary M, Goto J, Umemori H, Tezuka T, Iwakura Y, Watanabe M, Yamamoto T, Manabe T. EMBO J. 2006; 25:2867–2877. [PubMed: 16710293]
17. Miyakawa T, Yagi T, Kitazawa H, Yasuda M, Kawai N, Tsuboi K, Niki H. Science. 1997; 278:698–701. [PubMed: 9381182]
18. Yaka R, Phamluong K, Ron D. J Neurosci. 2003; 23:3623–3632. [PubMed: 12736333]
19. Wang J, Carnicella S, Phamluong K, Jeanblanc J, Ronesi JA, Chaudhri N, Janak PH, Lovinger DM, Ron D. J Neurosci. 2007; 27:3593–3602. [PubMed: 17392475]

20. Takagi N, Sasakawa K, Besshoh S, Miyake-Takagi K, Takeo S. J Neurochem. 2003; 84:67–76. [PubMed: 12485402]
21. Thornton C, Yaka R, Dinh S, Ron D. J Biol Chem. 2003; 278:23823–23829. [PubMed: 12695509]
22. Prybylowski K, Chang K, Sans N, Kan L, Vicini S, Wenthold RJ. Neuron. 2005; 47:845–857. [PubMed: 16157279]
23. Wechsler A, Teichberg VI. EMBO J. 1998; 17:3931–3939. [PubMed: 9670010]
24. Gurd JW, Bissoon N. J Neurochem. 1997; 69:623–630. [PubMed: 9231720]
25. Hisatsune C, Umemori H, Mishina M, Yamamoto T. Genes Cells. 1999; 4:657–666. [PubMed: 10620012]
26. Pickart CM. Annu Rev Biochem. 2001; 70:503–533. [PubMed: 11395416]
27. Fonseca R, Vabulas RM, Hartl FU, Bonhoeffer T, Nagerl UV. Neuron. 2006; 52:239–245. [PubMed: 17046687]
28. Ehlers MD. Nat Neurosci. 2003; 6:231–242. [PubMed: 12577062]
29. Patrick GN, Bingol B, Weld HA, Schuman EM. Curr Biol. 2003; 13:2073–2081. [PubMed: 14653997]
30. Colledge M, Snyder EM, Crozier RA, Soderling JA, Jin Y, Langeberg LK, Lu H, Bear MF, Scott JD. Neuron. 2003; 40:595–607. [PubMed: 14642282]
31. Sherman F. Methods Enzymol. 1991; 194:3–21. [PubMed: 2005794]
32. Thornton C, Tang KC, Phamluong K, Luong K, Vagts A, Nikanjam D, Yaka R, Ron D. J Biol Chem. 2004; 279:31357–31364. [PubMed: 15140893]
33. Ashique AM, Kharazia V, Yaka R, Phamluong K, Peterson AS, Ron D. Brain Res. 2006; 1069:31–38. [PubMed: 16414032]
34. Bradley J, Carter SR, Rao VR, Wang J, Finkbeiner S. J Neurosci. 2006; 26:1065–1076. [PubMed: 16436592]
35. Fuller KJ, Morse MA, White JH, Dowell SJ, Sims MJ. BioTechniques. 1998; 25:85–88. 90–82. [PubMed: 9668981]
36. Harrison SC. Cell. 2003; 112:737–740. [PubMed: 12654240]
37. Koo BK, Yoon KJ, Yoo KW, Lim HS, Song R, So JH, Kim CH, Kong YY. J Biol Chem. 2005; 280:22335–22342. [PubMed: 15824097]
38. Chung HJ, Huang YH, Lau LF, Huganir RL. J Neurosci. 2004; 24:10248–10259. [PubMed: 15537897]
39. Arundine M, Tymianski M. Cell Calcium. 2003; 34:325–337. [PubMed: 12909079]
40. Wu HY, Hsu FC, Gleichman AJ, Baconguis I, Coulter DA, Lynch DR. J Biol Chem. 2007; 282:20075–20087. [PubMed: 17526495]
41. Kassenbrock CK, Hunter S, Garl P, Johnson GL, Anderson SM. J Biol Chem. 2002; 277:24967–24975. [PubMed: 11994282]
42. Hegde AN, Goldberg AL, Schwartz JH. Proc Natl Acad Sci U S A. 1993; 90:7436–7440. [PubMed: 8395048]
43. Itoh M, Kim CH, Palardy G, Oda T, Jiang YJ, Maust D, Yeo SY, Lorick K, Wright GJ, Ariza-McNaughton L, Weissman AM, Lewis J, Chandrasekharappa SC, Chitnis AB. Dev Cell. 2003; 4:67–82. [PubMed: 12530964]
44. Chen W, Casey Corliss D. Dev Biol. 2004; 267:361–373. [PubMed: 15013799]
45. Choe EA, Liao L, Zhou JY, Cheng D, Duong DM, Jin P, Tsai LH, Peng J. J Neurosci. 2007; 27:9503–9512. [PubMed: 17728463]
46. Lai EC. Curr Biol. 2002; 12:R74–78. [PubMed: 11818085]
47. Fallon L, Moreau F, Croft BG, Labib N, Gu WJ, Fon EA. J Biol Chem. 2002; 277:486–491. [PubMed: 11679592]
48. Bingol B, Schuman EM. Nature. 2006; 441:1144–1148. [PubMed: 16810255]
49. Buttner C, Sadtler S, Leyendecker A, Laube B, Griffon N, Betz H, Schmalzing G. J Biol Chem. 2001; 276:42978–42985. [PubMed: 11560918]
50. Bedford FK, Kittler JT, Muller E, Thomas P, Uren JM, Merlo D, Wisden W, Triller A, Smart TG, Moss SJ. Nat Neurosci. 2001; 4:908–916. [PubMed: 11528422]

51. Kato A, Rouach N, Nicoll RA, Bredt DS. Proc Natl Acad Sci U S A. 2005; 102:5600–5605. [PubMed: 15809437]
52. Martin S, Nishimune A, Mellor JR, Henley JM. Nature. 2007; 447:321–325. [PubMed: 17486098]
53. Yi JJ, Ehlers MD. Pharmacol Rev. 2007; 59:14–39. [PubMed: 17329546]
54. Gutala R, Wang J, Kadapakkam S, Hwang Y, Ticku M, Li MD. Alcohol Clin Exp Res. 2004; 28:1779–1788. [PubMed: 15608593]
55. Moore DJ, West AB, Dawson VL, Dawson TM. Annu Rev Neurosci. 2005; 28:57–87. [PubMed: 16022590]
56. Ron D. Neuroscientist. 2004; 10:325–336. [PubMed: 15271260]
57. Coyle JT, Tsai G, Goff D. Ann N Y Acad Sci. 2003; 1003:318–327. [PubMed: 14684455]
58. Kemp JA, McKernan RM. Nat Neurosci. 2002; 5(suppl):1039–1042. [PubMed: 12403981]
59. Planells-Cases R, Lerma J, Ferrer-Montiel A. Curr Pharm Des. 2006; 12:3583–3596. [PubMed: 17073661]
60. Pace MC, Mazzariello L, Passavanti MB, Sansone P, Barbarisi M, Aurilio C. J Cell Physiol. 2006; 209:8–12. [PubMed: 16741973]

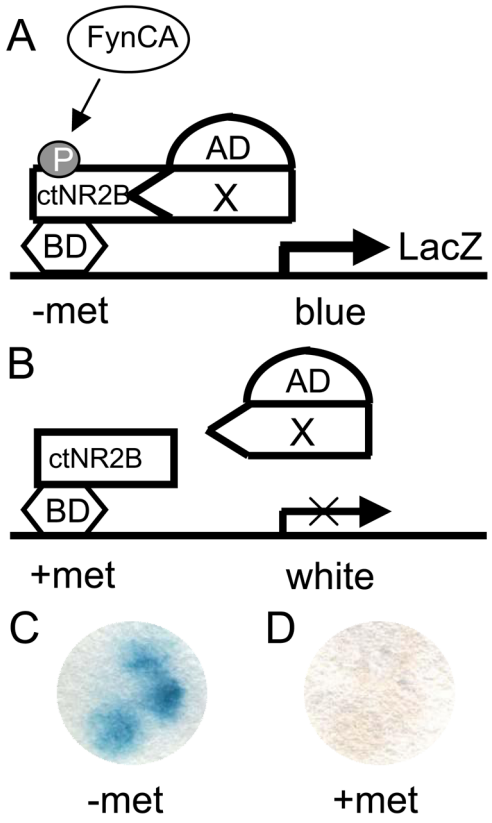

FIGURE 1. Yeast three-hybrid screen to identify Fyn phosphorylation-dependent NR2B interactants

Yeast were co-transformed with a rat brain cDNA library and a bait plasmid that expressed the cytoplasmic tail of the NR2B subunit of the NMDAR (*ctNR2B*) in-frame with a Gal4 DNA binding domain (*BD*) and a constitutively active form of Fyn (*FynCA*). FynCA expression was governed by a conditional methionine promoter, such that FynCA expression was induced in the absence of methionine (−*met*) (*A*) and repressed in the presence of methionine (+*met*) (*B*) in the yeast growth media. Colonies turning *blue* in the absence of methionine (*C*), but not in the presence of methionine (*D*), were identified as potential three-hybrid interactants reliant on the expression of FynCA.

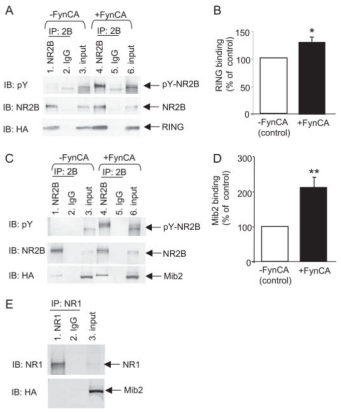

FIGURE 2. Mib2 interaction with the NR2B subunit of the NMDAR is enhanced in a Fyn phosphorylation-dependent manner

HEK293 cells were transiently transfected with plasmids encoding (*A*) the RING domain of Mib2 (*HA-RING*), and GFP-NR2B in the presence/absence of a plasmid encoding constitutively-active Fyn kinase (±*FynCA*), or (*C*) full-length Mib2 and GFP-NR2B in the presence/absence of FynCA. Immunoprecipitations (*IP*s) were carried out on total cell lysates (500 μg) using anti-NR2B (goat) antibodies or IgG antibodies as control. Immune complexes were detected by Western blotting using anti-NR2B (rabbit), HA (rat), and phosphotyrosine (pY) antibodies. Inputs are 5% of total lysate. *B* and *D*, quantitation of the band intensity of RING or Mib2 binding in the presence of FynCA (normalized to NR2B IP levels) are plotted as mean ± S.E., compared with the amount of binding in the absence of FynCA. *, $p < 0.05$; $n = 5$; **, $p < 0.01$, $n = 9$ (one sample *t* test). *E*, HEK293 cells were transiently transfected with plasmids encoding HA-Mib2 and NR1. IPs were performed on total cell lysates (500 μg) using anti-NR1 (mouse) antibodies and IgG (mouse) as control. Immune complexes were detected by Western blotting using anti-NR1 (mouse) and HA antibodies. Inputs are 5% of total lysate.

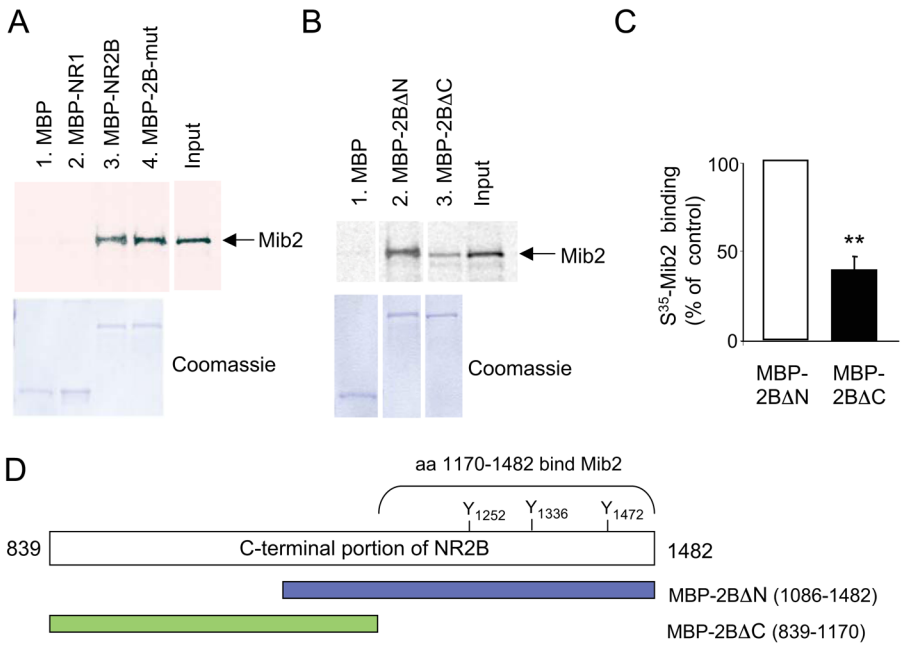

FIGURE 3. Mib2 interacts directly with NR2B

A, radiolabeled Mib2 (^{35}S-Mib2) was generated by *in vitro* translation using full-length Mib2 cDNA. ^{35}S-Mib binds to the cytoplasmic tail of maltose-binding protein-tagged NR2B (MBP-NR2B, *lane 3*), but not to MBP (*lane 1*) or to the cytoplasmic tail of the NR1 subunit (MBP-NR1, *lane 2*). It also binds to a phosphomimic mutant of NR2B (MBP-2B-mut, *lane 4*) in which the three main tyrosine residues for Fyn phosphorylation (Tyr^{1252}, Tyr^{1336}, Tyr^{1472}) have been mutated to aspartic acid residues. ^{35}S-Mib2 (10% of that used in the binding assay) was loaded as input. Samples were loaded in duplicate followed by Coomassie staining (*bottom panel*) to verify that equivalent amounts of MBP fusion proteins were used in the binding assays. *B*, deletion constructs of NR2B reveal that ^{35}S-Mib binds to the distal part of the cytoplasmic tail of NR2B (MBP-2BΔN, *lane 2*) and less well to the proximal portion of the NR2B tail (MBP-2BΔC, *lane 3*). Coomassie-stained gel (*bottom panel*) demonstrates that equivalent amounts of MBP fusion proteins were used in the binding assays. *C*, quantitation of the binding of ^{35}S-Mib to MBP-2BΔC compared with the binding of ^{35}S-Mib to MBP-2BΔN (normalized to 100%). **, $p < 0.01$, $n = 9$ (one sample *t* test). *D*, schematic diagram illustrating the MBP-2BΔN (1086 –1482 aa) and MBP-2BΔC- (839 –1170) NR2B protein fragments that were expressed, as well as the sites of the three tyrosine residues that were mutated within the NR2B tail.

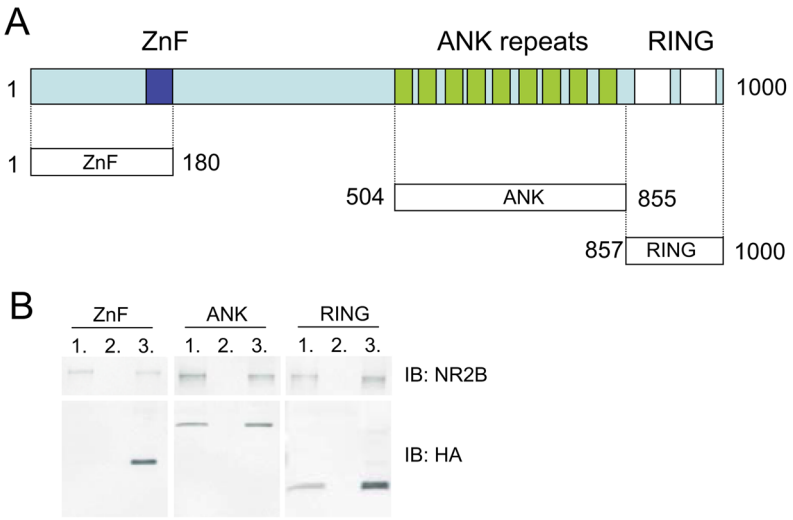

FIGURE 4. Identification of the domains of Mib2 that interact with the NR2B subunit

A, full-length Mib2 consists of a ZZ zinc finger domain (*ZnF*), ankyrin repeats (*ANK*), and RING finger domains (*RING*). Expression constructs consisting of regions encoding these domains were generated as indicated. *B*, HEK293 cells were transiently transfected with plasmids encoding GFP-NR2B and HA-tagged ZnF, ANK, and RING domains of Mib2. Immunoprecipitations (*IP*s) were carried out on total cell lysates (500 μg) using anti-NR2B (*lane 1*) and IgG (*lane 2*) goat antibodies. *Lane 3* depicts input samples (5% of total lysates). Immune complexes were detected by Western blotting using anti-NR2B (rabbit) and HA (rat) antibodies; $n = 3$.

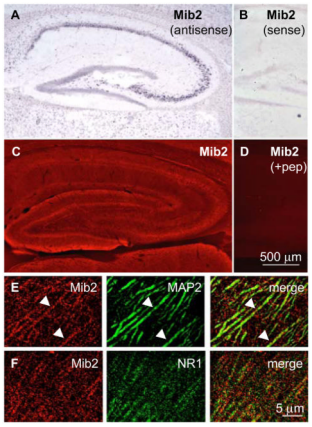

FIGURE 5. Mib2 is expressed in rat hippocampus

A and *B*, *in situ* hybridization using Mib2 (*A*) antisense and (*B*) sense probes in rat hippocampus. *C–F*, rat brain sections were immunostained using anti-Mib2 antibodies and (*D*) preincubation with Mib2 peptide antigen, or co-immunostained for (*E*) MAP2 or (*F*) NR1.

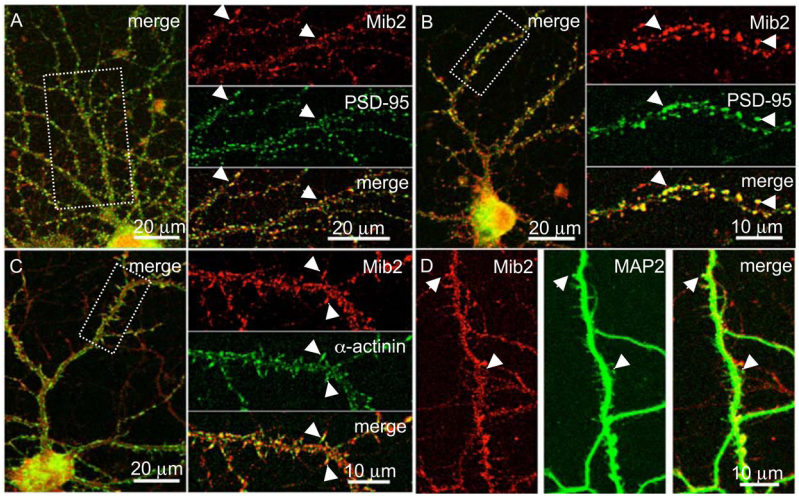

FIGURE 6. Mib2 is localized to postsynaptic sites in rat hippocampal neurons

Primary hippocampal cultures (21 days *in vitro*, d.i.v.) were immunostained for Mib2 and (*A* and *B*) PSD-95, (*C*) *α*-actinin or (*D*) MAP2.

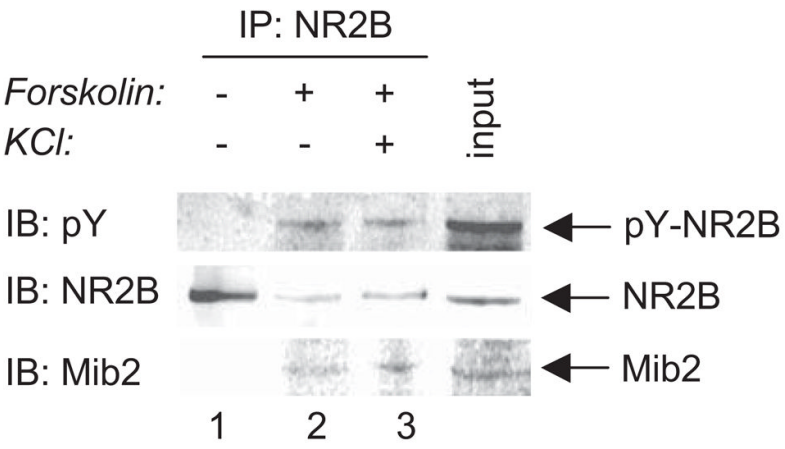

FIGURE 7. Mib2 associates with the NR2B subunit in the hippocampus

Rat hippocampal slices were treated with vehicle (*lane 1*), with forskolin (10 μ_M) for 15 min (*lanes 2* and *3*), or in the presence of KCl (50 m_M) added at the last 5 min of forskolin treatment (*lane 3*). IPs were performed on homogenates with anti-NR2B (goat) antibodies and probed with anti-NR2B (goat), Mib2 (mouse) and phospho-tyrosine (pY) antibodies. Input is 5% of homogenate.

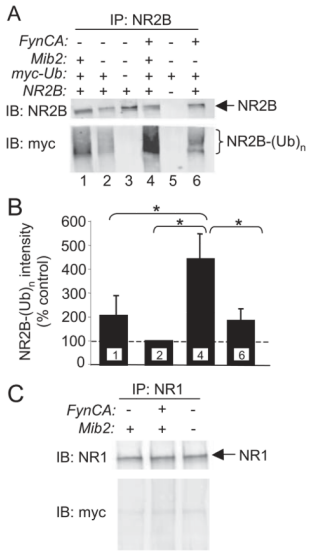

FIGURE 8. Mib2 ubiquitinates the NR2B subunit in a Fyn phosphorylation-dependent manner

A, HEK293 cells were transiently transfected with the following plasmids: FynCA, HA-Mib2, Myc-Ub, and GFP-NR2B. 48 h post-transfection, cells were treated with MG-132 (42 μM) for 3 h. IPs were carried out on total cell lysates (500 μg) using anti-NR2B (goat) antibodies. Immune complexes were detected by Western blotting using anti-NR2B (rabbit) and Myc antibodies to detect NR2B and NR2B-ubiquitinated species [NR2B-$(Ub)_n$], respectively. *B*, quantification of the intensity of NR2B-$(Ub)_n$ normalized to NR2B-IP levels. Values are plotted as mean ± S.E., with the amount of NR2B-$(Ub)_n$ observed in the absence of FynCA and Mib2 (*lane 2*) taken to be 100%. *, $p < 0.05$ (one-way analysis of variance); $n = 5$ (*lane 1*), and 6 (all other lanes). *C*, HEK293 cells were transiently transfected with HA-Mib2, myc-Ub, NR1, and FynCA. 48 h post-transfection, cells were treated with MG-132 (40 μM) for 3 h. IPs were carried out on total cell lysates (500 μg) using anti-NR1 (mouse) antibodies. Immune complexes were detected by Western blotting using anti-NR1 (goat) and Myc antibodies to detect NR1 and NR1-ubiquitinated species, respectively. $n = 3$.

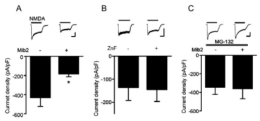

FIGURE 9. Expression of Mib2 depresses NR2B-containing NMDAR channel function in a ubiquitin-dependent manner

A, expression of Mib2 decreases the density of NMDA-elicited currents in HEK293 cells transfected with NR1 and NR2B subunits. The current density (pA/pF) was calculated as the peak amplitude of initial currents (pA) divided by the capacitance (pF) of cell membranes. *Inset*, sample traces of NMDA-evoked currents (5 s, 1 mM NMDA plus 50 μM glycine); *bar* indicates NMDA application. Calibration, 2 s, 100 pA/pF. *, $p < 0.05$ ($n = 13$ and 12 cells for cells with and without Mib2 expression, respectively, Student's *t* test). *B*, expression of a deletion mutant of Mib2 (ZnF) that does not bind NR2B does not affect NMDA-elicited currents ($n = 12$ and 11 for cells with and without ZnF expression, respectively). *C*, inhibition of the proteasome prevents the Mib2-induced decrease in the density of NMDA-elicited currents. HEK293 cells transfected with and without Mib2 were treated with the proteasome inhibitor, MG-132 (10 μM), for 2–3 h before recordings ($n = 14$ and 13 for cells with and without Mib2, respectively).